On the origin of whistler mode radiation in the plasmasphere

James L. Green,[1] Scott Boardsen,[2] Leonard Garcia,[3] W. W. L. Taylor,[3] Shing F. Fung,[1] and B. W. Reinisch[4]

Received 24 March 2004; revised 5 November 2004; accepted 26 November 2004; published 2 March 2005.

[1] The origin of whistler mode radiation in the plasmasphere is examined from 3 years of plasma wave observations from the Dynamics Explorer and the Imager for Magnetopause-to-Aurora Global Exploration spacecraft. These data are used to construct plasma wave intensity maps of whistler mode radiation in the plasmasphere. The highest average intensities of the radiation in the wave maps show source locations and/or sites of wave amplification. Each type of wave is classified on the basis of its magnetic latitude and longitude rather than any spectral feature. Equatorial electromagnetic (EM) emissions ($\sim$30–330 Hz), plasmaspheric hiss ($\sim$330 Hz to 3.3 kHz), chorus ($\sim$2–6 kHz), and VLF transmitters ($\sim$10–50 kHz) are the main types of waves that are clearly delineated in the plasma wave maps. Observations of the equatorial EM emissions show that the most intense region is on or near the magnetic equator in the afternoon sector and that during times of negative B_z (interplanetary magnetic field) the maximum intensity moves from L values of 3 to <2. These observations are consistent with the origin of this emission being particle-wave interactions in or near the magnetic equator. Plasmaspheric hiss shows high intensity at high latitudes and low altitudes (L shells from 2 to 4) and in the magnetic equator with L values from 2 to 3 in the early afternoon sector. The longitudinal distribution of the hiss intensity (excluding the enhancement at the equator) is similar to the distribution of lightning: stronger over continents than over the ocean, stronger in the summer than in the winter, and stronger on the dayside than on the nightside. These observations strongly support lightning as the dominant source for plasmaspheric hiss, which, through particle-wave interactions, maintains the slot region in the radiation belts. The enhancement of hiss at the magnetic equator is consistent with particle-wave interactions. The chorus emissions are most intense on the morningside as previously reported. At frequencies from $\sim$10 to $\sim$50 kHz, VLF transmitters dominate the spectrum. The maximum intensity of the VLF transmitters is in the late evening or early morning with enhancements all along L shells from 1.8 to 3.

Citation: Green, J. L., S. Boardsen, L. Garcia, W. W. L. Taylor, S. F. Fung, and B. W. Reinisch (2005), On the origin of whistler mode radiation in the plasmasphere, *J. Geophys. Res.*, *110*, A03201, doi:10.1029/2004JA010495.

1. Introduction

[2] Whistler mode radiation consists of electromagnetic waves whose upper frequency cutoff is either the local electron plasma frequency (f_p) or gyrofrequency (f_g), whichever is less [*Stix*, 1992]. Because of the large cold plasma density in the plasmasphere, f_p is greater than f_g and supports whistler mode radiation up to frequencies >50 kHz. In the plasmasphere the main whistler mode waves include equatorial electromagnetic (EM) emissions, plasmaspheric hiss, lightning whistlers, chorus, and VLF transmissions. An understanding of the whistler mode emissions in the plasmasphere is important in understanding the dynamics of the radiation belt electrons since the high-energy belt particles and the electromagnetic waves in the whistler mode frequency range are believed to strongly interact.

[3] Previous studies of the equatorial EM waves have been limited after first being pointed out by *Russell et al.* [1970]. The EM equatorial waves are believed to play an important role in transferring energy from energetic protons convecting earthward from the plasma sheet to the thermal plasmaspheric ions flowing along the geomagnetic field lines [*Gurnett*, 1976; *Boardsen et al.*, 1992]. To date, there has been no systematic spatial distribution study of these waves based on intensity and thereby no real context to understand where in the plasmasphere these potential particle-wave interactions may occur. This study addresses this issue.

[4] Plasmaspheric hiss is a broad diffuse band of electromagnetic radiation in the hundreds of hertz to 4 kHz frequency range that is confined to the plasmasphere [*Taylor*

[1]NASA Goddard Space Flight Center, Greenbelt, Maryland, USA.
[2]L3 Communications Analytics Division, NASA Goddard Space Flight Center, Greenbelt, Maryland, USA.
[3]QSS Group, Inc., Lanham, Maryland, USA.
[4]Center for Atmospheric Research, University of Massachusetts, Lowell, Massachusetts, USA.

0148-0227/05/2004JA010495$09.00

and Gurnett, 1968; *Russell et al.*, 1969; *Dunckel and Helliwell*, 1969]. Two of the most important characteristics of plasmaspheric hiss are its source location and generation mechanism. Even after 3 decades of space plasma wave research these two characteristics are still controversial, although significant progress has been made in their understanding. This controversy is explored further in this paper. The last comprehensive review of plasmaspheric hiss was done by *Hayakawa and Sazhin* [1992].

[5] Lightning generates a very broad emission spectrum. In the kilohertz frequency range, lightning waves are initially trapped in the waveguide formed by the lower ionosphere and ground, producing what are called sferics. Under certain conditions, at the atmospheric/ionospheric interface, wave energy can be transmitted through the ionosphere and into the plasmasphere where these waves propagate nearly along geomagnetic field lines in the whistler mode. As they propagate, they suffer dispersion, giving the well-known ''whistler'' spectrum [*Storey*, 1953]. These waves have been observed to directly interact with radiation belt electrons, causing them to precipitate [see, e.g., *Inan et al.*, 1989]. *Sonwalkar and Inan* [1989] were the first to observe lightning-generated whistlers triggering hiss emissions. This led these authors to the conclusion that lightning served, to an unknown extent, as an embryonic source of plasmaspheric hiss. This paper explores the relationship between the distribution of lightning on the Earth and the distribution of plasmaspheric hiss to determine the extent of the hiss-lightning relationship.

[6] Whistler mode chorus emissions are observed, extending from the outer regions of the plasmasphere/plasmapause and into the inner magnetosphere. *Sazhin and Hayakawa* [1992] reviewed chorus emissions, but a considerable amount of research has been accomplished since then. Much of the new research has explored the interaction with outer radiation belt electrons and chorus observed during substorms [see, e.g., *Meredith et al.*, 2000, 2002]. The spatial extent of these emissions is explored in this paper and is compared to previous results.

[7] A large number of VLF transmitters have been established by a number of countries for the purposes of navigation and communication. The frequencies of these transmitters range from as low as 10 kHz to as high as 50 kHz. Like lightning, transmitter waves also couple through the ionosphere to the magnetosphere and are trapped in the plasmasphere. Transmitter signals are also known to precipitate low-energy radiation belt electrons with energies <50 keV in the slot region between the inner and outer electron radiation belts [see, e.g., *Imhof et al.*, 1981; *Vampola*, 1977; *Inan and Helliwell*, 1982]. The spatial extent of VLF transmitter signals found in the plasmasphere is examined in this study.

[8] In order to perform a comprehensive spatial distribution of these whistler mode emissions a large plasma wave database has been developed. Very high quality plasma wave measurement data from a variety of instruments are now in the NASA National Space Science Data Center (NSSDC) archive. When properly combined into a three-dimensional database, these measurements can be used to construct intensity wave maps that yield statistically important source region information that may have been impossible to recognize previously. A similar approach to developing a model of the whistler mode wave activity in the plasmasphere has already been accomplished by *André et al.* [2002], using the same archival Dynamics Explorer 1 (DE)/plasma wave instrument (PWI) data. However, that study did not take into account local time variations in producing latitudinal distributions [see *André et al.*, 2002, Figures 4 and 5], and no attempt was made to look for any geographic control of these whistler mode waves indicating a lightning origin.

[9] With the plasma wave intensity map technique we now have the ability to globally analyze the intensity of plasmaspheric whistler mode waves in a quantitative and systematic fashion, thereby putting into context their spatial distribution and intensity. We look for ''hot spots'' in the average wave intensities, thereby identifying source regions and/or sites of plasma wave amplification. The purpose of this paper is to use this new wave map technique to apply a classification scheme for whistler mode waves on the basis of the similarity of their spatial distributions with frequency in a way that has not been presented by earlier studies. This unique approach focuses more on classifying the waves by a common origin rather than by previous spectral analysis taken at any one location in the plasmasphere and will more easily provide a method to determine the source region of these whistler mode waves in the plasmasphere.

2. Observations

[10] Observations used in this study are from the PWI on the DE mission [*Shawhan et al.*, 1981] and the radio plasma imager (RPI) on the Imager for Magnetopause-to-Aurora Global Exploration (IMAGE) mission [*Reinisch et al.*, 2000]. DE was launched on 3 August 1981 into a polar orbit with initial apogee of 4.65 Earth radii (R_E) geocentric radial distance and 675 km perigee altitude with an orbital period of 6.8 hours. The orbital precession of 108°/yr allowed DE to cross the plasmasphere at all local times and nearly all latitudes over a 3 year period. Data from the DE/PWI used in this study are from the period from 16 September 1981 to 23 June 1984. DE/PWI data were received ~40% of the time because of telemetry coverage. The PWI makes spectral measurements over a frequency range from 1.8 Hz to 400 kHz using the sweep frequency receiver. The measurements are made in 1% frequency bands, logarithmically spaced in frequency. All the DE/PWI data are available in the NSSDC. Four consecutive amplitude measurements for the electric and magnetic wave receivers at each frequency step along with time, frequency, antenna connection, and spacecraft position information are available in the archive. Only the second of the four consecutive amplitude measurements is used. The DE/PWI electric field measurements used in this study are all from the 200 m tip-to-tip wire antenna and the 1 m square loop antenna for simultaneous magnetic wave measurements.

[11] The IMAGE spacecraft was launched on 25 March 2000 into a highly elliptical polar orbit with initial geocentric apogee of 8.22 R_E and perigee altitude of 1000 km. The RPI instrument on IMAGE is a highly flexible radio sounder that transmits and receives coded radio frequency pulses in the frequency range from 3 kHz to 3 MHz. RPI also makes passive radio measurements (300 Hz bandwidth) that are used in this study. RPI utilizes three orthogonal

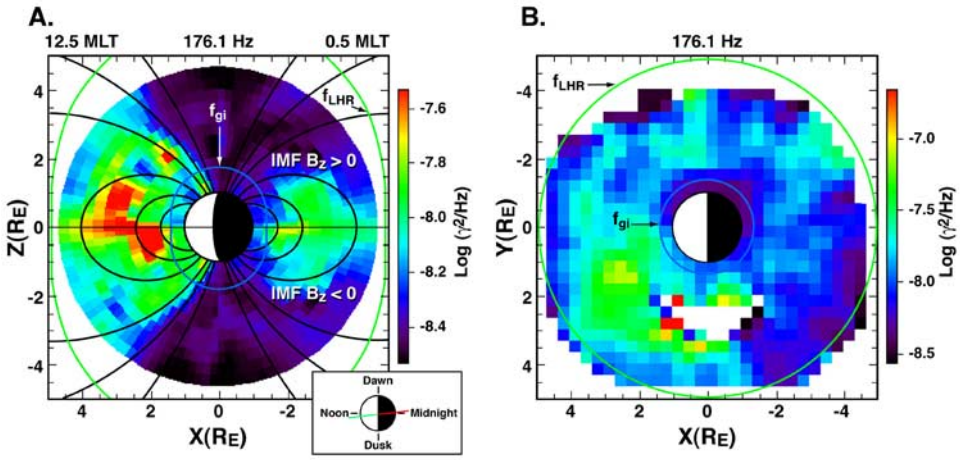

Figure 1. (a) Latitudinal and (b) local time distributions of the average magnetic field spectral density of equatorial electromagnetic (EM) emissions in the plasmasphere. Closed L shells of 1.5, 3, and 4 are shown in Figure 1a along with field lines at 70°, 75°, and 80°.

dipole antennas of 325 m (x axis), 500 m (y axis), and 20 m (z axis), all tip-to-tip lengths. The x axis antenna was 500 m at the beginning of the mission but was shortened to 325 m when it apparently collided with micrometeoroid or orbital debris on 3 October 2000. The IMAGE data coverage is from 1 January 2001 to 6 August 2003. Telemetry coverage of RPI was above 95% during this interval. The IMAGE/RPI and IMAGE orbit data are archived at the NSSDC. Eight consecutive amplitude measurements (3.2 ms/sample) for the electric wave receiver at each frequency step from each antenna along with time, frequency, antenna connection, and spacecraft position information are available in the archive. Only the first of the eight consecutive amplitude measurements from the x axis antenna is used.

[12] The wave map technique used in this study is similar to that used by *Green and Boardsen* [1999] in the study of continuum radiation. The PWI and RPI data were separated into bins of 5° in geomagnetic latitude and 12° in geomagnetic longitude for all radial distances <3.5 R_E, saving the total of the log of the spectral density and total numbers of measurements in each bin for each frequency. No normalization of spectral power densities as a function of radius or distance along a flux tube was attempted. Wave map movies were generated for each frequency for the PWI and RPI data. The data values used for each bin in the wave maps are a weighted average over a bin and its eight nearest neighbors (total spectral density summed over nine bins divided by the total number of individual measurements summed over the nine bins).

[13] Within the plasmasphere, in addition to radiation in the electromagnetic whistler mode, strong low-frequency electrostatic emissions are also prevalent. Only the DE magnetic wave measurements will be used for the whistler mode waves at low frequencies. This will avoid adding the unwanted intensities of electrostatic emissions into the wave survey for those frequencies. This procedure will ensure that only the whistler mode waves are included.

2.1. Equatorial EM Emissions

[14] The average DE/PWI magnetic field spectral densities in the 176.1 Hz band are shown in Figure 1, where Figure 1a is a plot of measurements in the 1230–0030 magnetic local time (MLT) meridian plane and Figure 1b is a plot of measurements in the equatorial plane for the same frequency band in solar magnetospheric coordinates. White pixels indicate no DE measurements. The wave measurements for Figure 1a are sorted by using the sign of the z component of the interplanetary magnetic field (IMF B_z). It is well known that the IMF B_z parameter is an important factor in the generation of geomagnetic substorms. In Figure 1a the average magnetic field spectral density is binned according to the absolute value of the magnetic latitude times the sign of the IMF B_z. Therefore the $+z$ axis in Figure 1a is the subset of observations for which IMF B_z is positive, while the $-z$ axis is the subset of observations for which the IMF B_z is negative. This method has a number of advantages and is applicable to whistler mode waves because of their expected generation and propagation symmetry about the magnetic equator.

[15] All the characteristic features of the magnetic field spectral density distributions shown in Figures 1a and 1b are also found over the entire frequency range from ~30 to ~330 Hz. This emission is equatorial EM (fast magnetosonic mode) radiation [*Russell et al.*, 1970; *Gurnett*, 1976; *Boardsen et al.*, 1992] and is found at frequencies between the proton gyrofrequency (f_{gi}) and the lower hybrid frequency (f_{LHR}). The f_{gi} and f_{LHR} frequencies are shown in Figure 1 in blue and green, respectively. Other labels such as the electron gyrofrequency (f_{ge}) are marked in red and are also used in the wave maps (not shown in Figure 1). The quantities f_{gi} and f_{ge} are calculated from the measured magnetic field on board DE and from a *Tsyganenko* [1995] model field for IMAGE. The f_{LHR} is estimated by using the geometric mean of f_{gi} and f_{ge} (which is the upper limit of the lower hybrid). The magnetic field of the EM waves is nearly aligned with the ambient magnetic field; therefore the wave vector is nearly perpendicular to the ambient magnetic field. The wave vector direction combined with the elongated shape of the index of refraction surface along the ambient magnetic field direction strongly confines these waves to the magnetic equatorial region as is

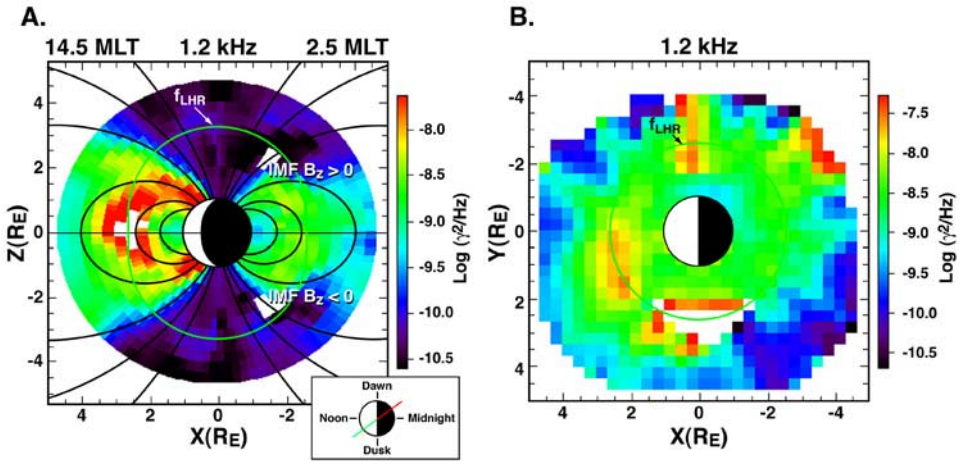

Figure 2. Same format as Figure 1 but primarily for plasmaspheric hiss. (a) Latitudinal distribution of the maximum intensity of the waves following midlatitude field lines. (b) Maximum intensity of plasmaspheric hiss occurring on the dayside. The emissions on the morningside are chorus.

demonstrated by cold plasma ray tracing [*Boardsen et al.*, 1992].

[16] This study provides, for the first time, a quantitative spatial distribution of the EM equatorial emissions in local time. The distribution of wave spectral densities shown in Figure 1a confirms previous studies of the near-equatorial nature of these waves in the outer plasmasphere. In addition, Figure 1a strongly suggests that particle-wave interactions occur within a few tens of degrees of the magnetic equator over a large range in radial distance, 1.5–4 R_E geocentric radial distance, and that specific L shells for both positive and negative B_z values (nonstorm and storm conditions) have the highest intensities of the emission. Figure 1b shows that the most intense portion of the equatorial EM emissions is located in the middle to late afternoon local time region and that the emission is rarely measured in the premidnight sector. Previous results have left the impression that the EM equatorial emissions have, according to *Gurnett* [1976, p. 2766], "no marked dependence on local time".

2.2. Plasmaspheric Hiss

[17] The plasma wave magnetic spectral density maps for plasmaspheric hiss near its spectral peak between 1 and 2 kHz are shown in Figure 2. Although found essentially everywhere in the plasmasphere at some intensity, plasmaspheric hiss is most intense throughout the local afternoon sector (see Figure 2b) and on L shells which contain the slot region in the electron radiation belts (see Figure 2a). In the frequency range from ~330 Hz to ~3.3 kHz both magnetic meridian and equatorial plane plasma wave magnetic field spectral density maps from PWI data show essentially the same distributions as in Figure 2 for 1.2 kHz. Over the frequency range from 2.7 to 3.3 kHz the intensity and spatial extent of the emission decrease significantly. The transition from the EM equatorial emission to plasmaspheric hiss occurs over the frequency range from ~230 to ~380 Hz. The wave activity in Figure 2b occurring in the early morning and near-dawn sector is just the beginning of the chorus emissions that are discussed in section 2.3.

[18] It is important to note that in the frequency range from ~330 Hz to ~3.3 kHz several emissions are observed in the plasmasphere such as plasmaspheric hiss, whistlers, and chorus. The DE/PWI instrument has a bandwidth of 1% and a time resolution of 1 s/32 channels; when combined with the wave map technique used in this study, the results are not sufficient to resolve the plasma wave observations into discrete whistlers. Whistlers are most commonly observed by instruments giving superior time and frequency resolution and typically equipped with automatic gain control capabilities, all of which enable discrete emissions such as whistlers to be captured. Therefore the results of this study, by their nature, emphasize observations of broadbanded emissions that are much more continuous in time (i.e., plasmaspheric hiss) than are the discrete lightning whistler emissions. The identification of the plasmaspheric hiss is uniquely done from the spatial distribution in magnetic latitude and local time at each frequency. The similarity of this distribution over a number of consecutive frequency channels significantly supports the identification of the emission as plasmaspheric hiss.

[19] It is important to note that these distributions are smoothed and by their nature would only show geomagnetic storm time differences if the latitudinal structures changed significantly as in the case of the equatorial EM radiation shown in Figure 1. Since there is no significant change in the latitudinal distribution of plasmaspheric hiss, as shown in Figure 2, storm time intensifications that have been reported by *Larkina and Likhter* [1982] are therefore all averaged together.

[20] The waves that *Thorne et al.* [1973, p. 1581] describe as plasmaspheric hiss and that "appear to be continuously present throughout the plasmasphere at all latitudes and longitudes" may actually be a combination of both equatorial EM radiation and plasmaspheric hiss as described in this paper. Although similar in MLT distribution as shown in Figures 1b and 2b, the latitudinal distributions (Figures 1a and 2a) show a significantly different distribution. It is only through this wave map technique that we are able to clearly distinguish between these two types of whistler mode radiation.

[21] It is important to note that in the recent paper by *Meredith et al.* [2004], wave maps of plasmaspheric hiss

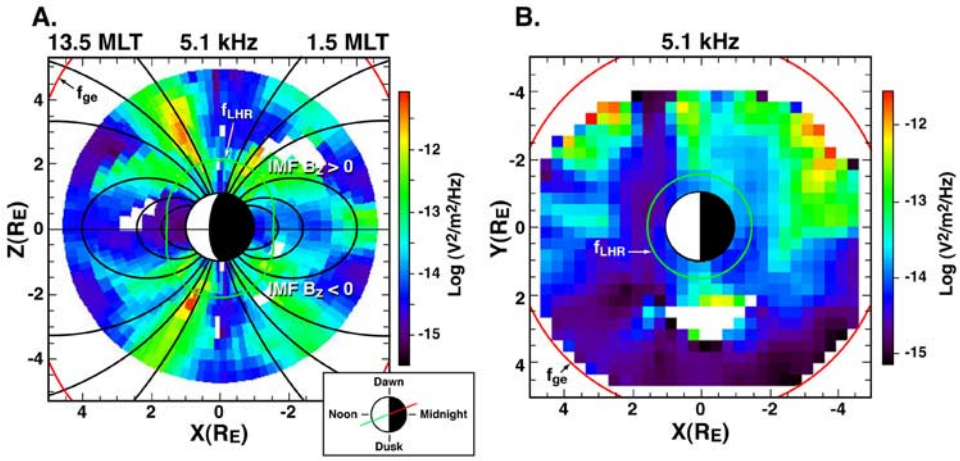

Figure 3. Same format as Figure 1 but showing the electric field intensity for 5.1 kHz. (a) Whistler mode waves in the polar cusp (on the dayside at high L values), in the auroral zone (on the nightside), and in the magnetic equator on the nightside (chorus). (b) Chorus emissions showing the broad spatial distribution extending from early morning hours to nearly noon.

were generated by combining all data from frequencies between 0.1 and 2 kHz. We believe that their technique potentially combines some of the equatorial EM emissions with plasmaspheric hiss. As clearly demonstrated in this paper, the EM emissions dominate the spectrum in the frequency range up to ~330 Hz and have significantly different spatial distributions relative to plasmaspheric hiss and to substorm parameters (IMF B_z).

2.3. Chorus

[22] Whistler mode chorus observations are from near the plasmapause and to greater radial distances. Figure 3 is in the same format as Figure 1 but shows the electric field intensity for 5.1 kHz. Figure 3a shows the whistler mode waves in the polar cusp (on the dayside at high L values), in the auroral zone (on the nightside), and in the magnetic equator on the nightside (chorus waves). The chorus emissions are further illustrated in Figure 3b, showing the broad spatial distribution extending from early morning hours to nearly noon. The distribution of chorus as shown in Figure 3 is nearly identical to that reported by *Koons and Roeder* [1990] and *Summers et al.* [1998]. Using the wave map technique, similar spatial distributions of chorus extend from ~1.2 to ~6 kHz in frequency.

[23] Chorus emissions are characterized as discrete emissions usually rising rapidly in frequency with time. Typically, a large number of these discrete emissions are observed together and are often observed with a band of hiss emissions [*Koons*, 1981]. These two factors contribute to chorus emissions being clearly identified on a number of sweep frequency receiver systems [see, e.g., *Horne et al.*, 2003] in addition to wideband instruments [*Santolik et al.*, 2004], therefore allowing us to be able to identify at least the most intense chorus distributions in the wave map study presented here.

2.4. Ground Transmitters

[24] VLF ground transmitters operate over the frequency range from ~10 to 50 kHz with a narrow bandwidth (usually <1 kHz) and generate wave energy that typically couples into the plasmasphere in the whistler mode. Figure 4 is in the same format as Figures 1 and 2 but illustrates magnetic field spectral densities at 11.8 kHz and with f_{ge} and f_{LHR} indicated by red and green lines, respectively. The distribution shown in Figure 4 is similar to those at frequencies of all other ground transmitters from 10 to 50 kHz. Figure 4a shows the latitudinal distribution of the magnetic field spectral density of the waves that follow midlatitude field lines. Figure 4b shows that the maximum magnetic field spectral density of waves from ground transmitters occurs on the nightside. It is important to note the similarity in the latitudinal distribution of plasmaspheric hiss (Figure 2) and that of transmitters (Figure 4), even though the most intense portions of these waves have different local time distributions.

[25] The electric field spectral densities from IMAGE/RPI of three ground transmitters operating in the United States (two, designated by call letters NLK and NML, known to us and one unknown) at 25.0 kHz are shown in Figure 5. Figures 5a and 5c illustrate data selected from the 1400–1800 and 0200–0600 MLT sectors, respectively, as shown in Figure 5b, which is in the same local time distribution format as that presented at 11.8 kHz in Figure 4. The electric field wave measurements in Figures 5a and 5c are mapped to geographic coordinates along the associated geomagnetic field lines. Electric field wave measurements within 10° of the magnetic equator or in locations in which the gyrofrequency was less than the wave frequency were excluded. This criterion was necessary to ensure that only whistler mode waves were included and that the appropriate mapping along field lines was accomplished to keep the Northern and Southern Hemisphere distributions separate. The magnetic conjugate points of the transmitters are shown as white circles.

[26] Figure 5 shows the broad, tens of degrees extent of the transmitter radiation, which couples from the ground into the plasmasphere. Figure 5 clearly shows that the transmitters' waves coupling into the plasmasphere are strongest on the nightside (Figure 5c) and weakest on the dayside (Figure 5a) where the extent of the coupling is

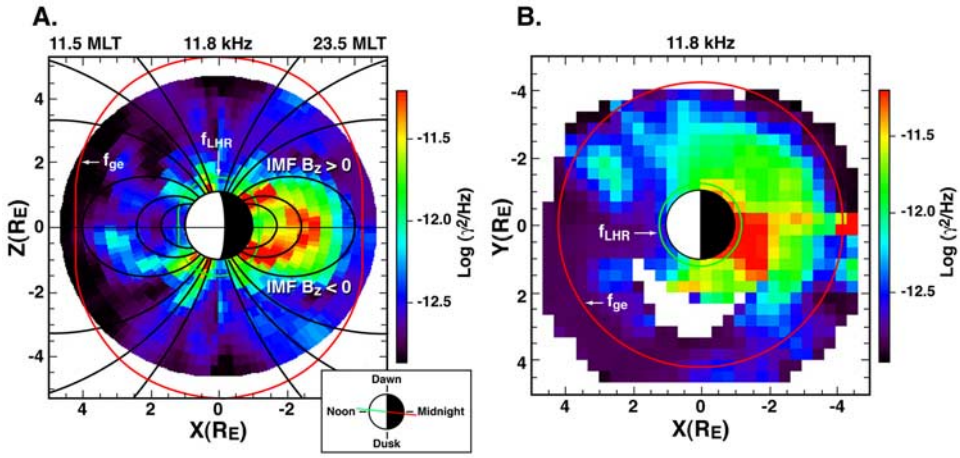

Figure 4. Same format as Figure 1 but for ground transmitters at 11.8 kHz. The intensity distribution shown is similar to all ground transmitters over the frequency range from ~10 to 50 kHz. (a) Latitudinal distribution of the maximum intensity of the waves following midlatitude field lines. (b) Maximum intensity of ground transmitters occurring on the nightside in the late evening and early morning sectors.

significantly less. In addition, the transmitter observations in Figure 5 show the confinement of the whistler mode waves to a longitude range of about 30°–40° on the dayside (Figure 5a) from its generation sites.

[27] It has been known for some time [*Helliwell*, 1965] that ionospheric absorption of VLF signals generated on the ground depends mainly upon the electron density and collision frequency (between electrons and neutrals) in the D layer. The D layer is the most extensive on the dayside since its dominant source is photoionization followed by precipitation (which is not significant at the midlatitudes where the ground transmitters mostly reside). Given that ground transmitters generate a constant source of waves with local time, the differences in the day-night distribution shown in Figure 5 are most likely due to the day-night asymmetry in the absorbing D layer.

3. Lightning as a Source of Plasmaspheric Hiss

[28] The classic theoretical work by *Kennel and Petschek* [1966] held that under certain circumstances, whistler mode waves increase in energy from a gyroresonance interaction

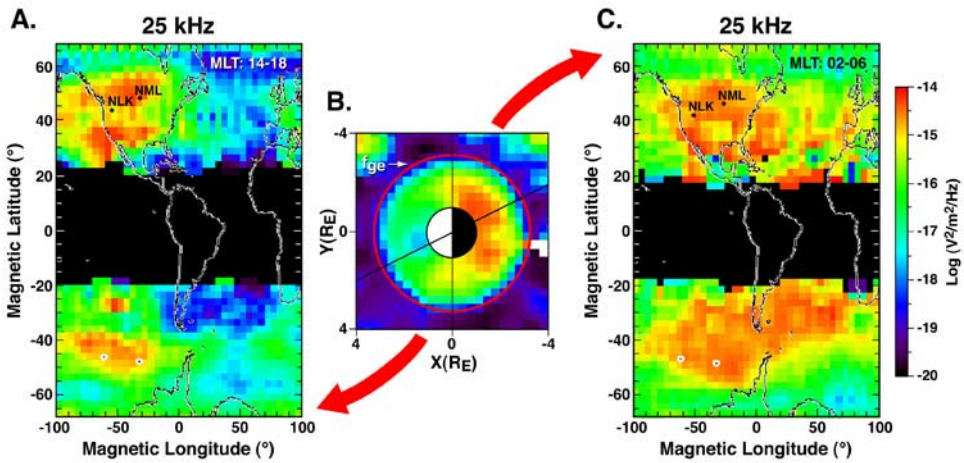

Figure 5. Average electric field wave spectral density from Imager for Magnetopause-to-Aurora Global Exploration (IMAGE)/radio plasma imager (RPI) measurements of several ground transmitters at 25.0 kHz. (a) Electric field wave measurements mapped to magnetic coordinates (with continents outlined) along field lines for 1400–1800 magnetic local time (MLT). (b) Same basic local time distribution as that presented at 11.8 kHz in Figure 4. (c) Same as Figure 5a but for 0200–0600 MLT. Electric field wave data that were within 10° of the magnetic equator or in locations in which the gyrofrequency was less than the wave frequency were excluded. Three ground transmitters are operating in the United States (two known and one unknown). The conjugate points of the known transmitters are shown as white circles. Transmitter radiation coupling from the atmosphere to the plasmasphere is the strongest on the nightside (Figure 5c).

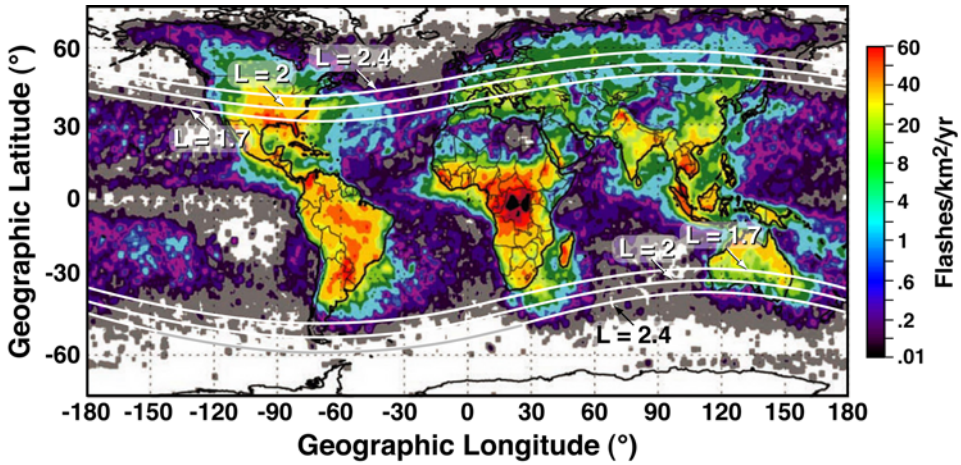

Figure 6. Annualized geographic distribution of lightning from *Christian et al.* [2003] and the main slot region L shells after *Rodger et al.* [2003]. Because of the tilt of the magnetic pole the regions of North America, Europe, Russia, and Australia provide the vast majority of lightning whistlers into the slot region.

with radiation belt electrons, causing the electrons to change pitch angle and to precipitate (pitch angle scattering). *Lyons et al.* [1972] and *Abel and Thorne* [1998a, 1998b] showed that plasmaspheric hiss would be the dominant whistler mode wave responsible for this scattering, thereby maintaining the electron slot region between the inner and outer electron belts. Therefore understanding the origin of hiss is of fundamental importance in understanding the distribution and dynamics of the electron radiation belts.

[29] The origin of plasmaspheric hiss is still somewhat controversial as being generated either by the above gyroresonance process [see, e.g., *Thorne et al.*, 1973; *Huang et al.*, 1983; *Church and Thorne*, 1983] or by lightning [*Sonwalkar and Inan*, 1989; *Draganov et al.*, 1992] or by both, but the relative contribution from these two sources is still unknown even though the literature in this field is extensive. *Thorne et al.* [1979] suggested that plasmaspheric hiss would only grow in intensity from the background thermal noise to its observed intensity from gyroresonance acceleration as the whistler mode wave repeatedly returned through the equator. On the basis of limited data, *Solomon et al.* [1988] have shown that amplification of background noise to observed hiss intensities is possible. In addition, from ray-tracing calculations of magnetospherically reflected whistlers, *Thorne and Horne* [1994] concluded that lightning-generated whistlers could not be the source of plasmaspheric hiss because they are subject to significant damping due to Landau resonant interactions with suprathermal electrons with energies greater than $\sim$100 eV.

[30] Observations from the low-frequency linear wave receiver on DE by *Sonwalkar and Inan* [1989] have shown that lightning-generated whistlers often trigger plasmaspheric hiss. These in situ observations were the first to demonstrate that lightning could be the original source of plasmaspheric hiss. Ray-tracing calculations by *Draganov et al.* [1992] demonstrated that the refraction of the plasmasphere on lightning whistlers (higher-frequency waves move to higher L shells) produced a natural way to obtain a hiss-like spectrum on lower L shells. In addition, *Draganov et al.* [1992] determined that the total wave energy from lightning whistlers may maintain the experimentally observed levels of plasmaspheric hiss.

[31] The wave-mapping technique used in section 2 is applied over the frequency range from 30 Hz to 50 kHz. The transmitter data presented in section 2.4 are used to set the context for analyzing the whistler mode waves at lower frequencies. The similarities in Figures 2a (hiss) and 4a (transmitters), showing that the most intense portions of the waves are along high-latitude magnetic field lines, suggest an Earth origin even though the local time distributions are different. These observations support the previous work by *Sonwalkar and Inan* [1989], *Draganov et al.* [1992], and *Bortnik et al.* [2003a] and provide the motivation to further explore the possibility of an Earth origin for hiss.

[32] In order to investigate what contribution lightning may play in providing whistler mode radiation to the plasmasphere, DE/PWI (30 Hz to 50 kHz) and IMAGE/RPI (3–50 kHz) data, separately and at each frequency, were remapped into geographic coordinates and were compared with the average distribution of lightning, creating a whole new series of wave maps for analysis. Like the transmitter data of Figure 5, the electric field wave measurements within 10° of the magnetic equator or in locations in which the gyrofrequency was less than the wave frequency were excluded. The data prepared in this way would then provide insight into the importance of lightning as a source of plasmaspheric hiss. Plasmaspheric hiss that grows in intensity because of particle-wave interactions from the background thermal noise, as suggested by *Thorne et al.* [1979], would have a distribution completely independent of any geographic mapping. In order for lightning to even be considered to be an element of plasmaspheric hiss a geographic relationship would have to be established between lightning and the observed distribution of plasmaspheric hiss.

[33] The average distribution of lightning strikes worldwide has been measured by the optical transient detector on board the MicroLab 1 satellite by *Christian et al.* [2003] and is shown in Figure 6 along with the main slot region L shells

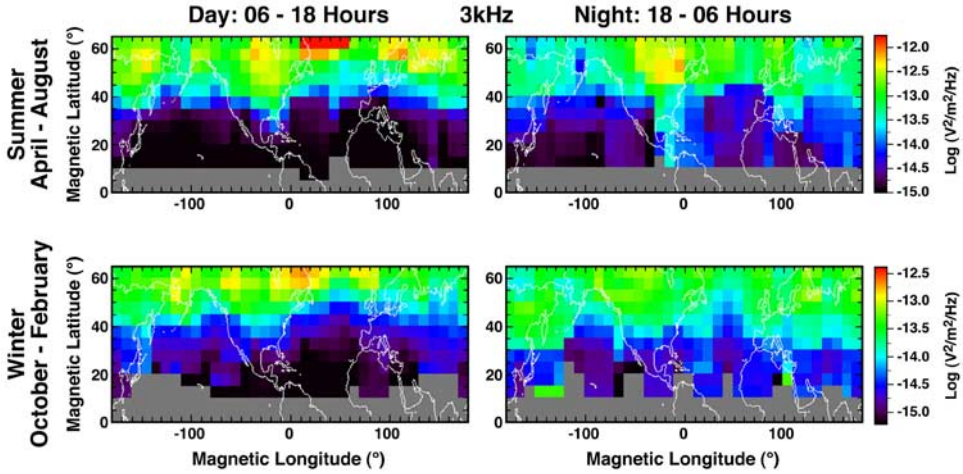

Figure 7. Average electric wave spectral density from all DE 1/plasma wave instrument data of plasmaspheric hiss mapped to geographic coordinates (in the same manner as Figure 5) at 3 kHz. (left) Dayside observations and (right) nightside observations. (top) Summer and (bottom) winter with the exclusion of the equinox months of March and September. Like the world distribution of lightning, the world distribution of plasmaspheric hiss follows the continents and is stronger on the dayside than on the nightside and is stronger in summer than in winter. The same distributions are also observed using the IMAGE/RPI data.

[after *Rodger et al.*, 2003]. Figure 6 is an annualized distribution of lightning clearly showing that the lightning distributions are largely confined to the continents. Because of the tilt of the magnetic pole the regions of North America, Europe, Russia, and Australia provide the vast majority of lightning whistlers into the slot region. *Christian et al.* [2003, Figure 7] also showed the seasonal lightning distributions. The seasonal distributions of lightning activity show significantly more lightning in the summer hemisphere than in the corresponding winter hemisphere. For instance, virtually no lightning is observed in the Northern Hemisphere during the months of December, January, and February. From an analysis of their annual lightning distributions, *Christian et al.* [2003] determined that lightning occurs mainly over land areas, with an average land/ocean ratio of 10:1. Statistically, these authors found that there is an average of 44 (±5) lightning flashes occurring around the globe every second. In another recent study of lightning, *Mazany et al.* [2002] measured the day-night effect at midlatitudes and found that as many as 10 times more lightning events occur in the postnoon than in the postmidnight sector.

[34] The average wave electric field spectral density from all DE/PWI measurements of plasmaspheric hiss mapped to magnetic coordinates with continents, at 3 kHz, is shown in Figure 7 (in a manner similar to the transmitter data in Figures 5a and 5c). Figure 7 (left) shows dayside observations, and Figure 7 (right) shows nightside observations. Figure 7 (top) shows summer, and Figure 7 (bottom) shows winter. The equinox months of March and September are excluded.

[35] The analysis of the resulting wave maps shows that the correspondence between the enhanced intensities and continents occurs over the ~500 Hz to ~3 kHz frequency range. This is almost identical to the frequency range of plasmaspheric hiss as determined from the spatial distributions presented in this study (see section 2.2 and Figure 2).

[36] Like the world distribution of lightning the world distribution of plasmaspheric hiss follows the continents, is stronger on the dayside than on the nightside, and is stronger in summer than in winter. The same distributions are also observed using the IMAGE/RPI data. The day-night asymmetry is also seen in Figure 2b.

[37] Electric field spectral density measurements and the major landmasses from Figure 7 at 45° invariant latitude (L = two-slot region) in the Northern Hemisphere are shown in Figure 8. Figure 8 provides quantitative measurements of the average electric field and allows for direct comparison of the summer/winter and day/night effects that Earth lightning exhibits. The summer data are shown in red, and the winter data are shown in blue. Peak intensities of plasmaspheric hiss are shown over land with minimums over the ocean and with summer observations being stronger than the observations during the winter. The average variation between the red and blue curves in both Figures 8a and 8b is ~1 order of magnitude. These results strongly suggest that lightning is the dominant source of plasmaspheric hiss.

[38] The observations in Figure 5 of radiation from ground transmitters clearly show peak intensities above the radiating stations and at their associated conjugate point. Assuming that waves from lightning also follow this pattern, it is important to consider how the lightning from the Southern Hemisphere would affect these observations. The winter (Northern Hemisphere) trace in Figure 8a shows a clear wave intensity peak from −150° to −110° magnetic longitude. This peak corresponds to the conjugate longitude of Australia, which is the only Southern Hemisphere continent on L shells that maps into the slot region and would be in its summer season where the peak in its thunderstorms

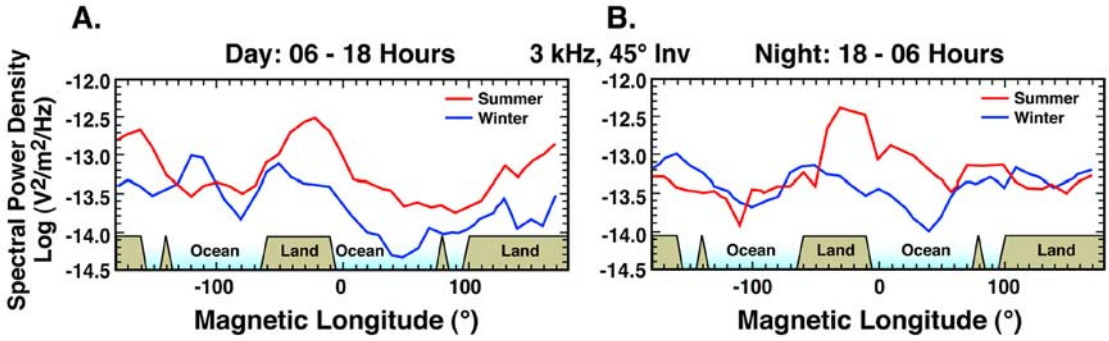

Figure 8. Electric field spectral density measurements and landmasses at 45° invariant latitude of data sorted in Figure 7. (a) Dayside and (b) nightside observations. The summer data are shown in red, and the winter data are shown in blue. Peak intensities of plasmaspheric hiss are over land with minimums over the ocean and with summer intensities being stronger than winter.

occurs. Once again, this provides more confidence in lightning as the primary source of plasmaspheric hiss.

4. Discussion

[39] If lightning is a major source of plasmaspheric hiss, as this study indicates, then why are the discrete frequencies characteristic of a plasmaspheric lightning whistler so different from the broad, featureless, variable intensity characteristic of plasmaspheric hiss? *Draganov et al.* [1992] used ray-tracing calculations to demonstrate the evolution of magnetospherically reflected whistler wave energy into hiss-like spectra via the settling of wave energy on specific L shells. Magnetospherically reflecting whistlers do not bounce off the plasmapause but are internally reflected within the plasmasphere. *Draganov et al.* [1992] found that the lightning-generated whistlers tend to settle on preferred L shells in the plasmasphere with the lower-frequency components settling on higher L shells and higher-frequency components settling on lower L shells. Their estimates of the resulting whistler mode energy from lightning discharges were comparable to experimentally observed levels of plasmaspheric hiss. By combining the lightning whistler lifetimes with the power spectral density of lightning, *Bortnik et al.* [2003b] showed a clear maximum in wave energy in the slot region at an L shell of about 2–3. This is very consistent with the observations presented in Figures 2a and 2b. *Sonwalkar and Inan* [1989] observed that lightning-generated whistlers often trigger hiss emissions. These observations led the authors to the conclusion that lightning served, to an unknown extent, as an embryonic source of plasmaspheric hiss. This paper puts the previous results described above into context and shows that lightning must be a major source of plasmaspheric hiss. Figure 8 shows that the geographic mapping of plasmasphere hiss is strikingly similar to lightning distributions for both day/night and summer/winter variability. The evidence is compelling and overwhelming.

[40] Previous researchers have tried to make the same connection. *Tsurutani et al.* [1979] searched for geographic dependence of plasmaspheric hiss at 550 Hz from the polar orbiting OGO 6. *Tsurutani et al.* [1979, p. 4116] concluded that from the "totality of satellite data analyzed to date . . . [the results are] consistent with a predominantly natural origin [nonlightning] for . . . plasmaspheric hiss." It is unfortunate that these authors did not look at higher frequencies since the strong geographic mapping of plasmaspheric hiss only becomes obvious above this frequency.

[41] The reason why the plasmaspheric hiss maps so well to the geography of land (Figure 6) is revealed by examining the day/night variation in longitude from the transmitter waves coupling into the plasmasphere (Figure 5). Unlike ground transmitters the most intense portion of plasmaspheric hiss occurs on the dayside (afternoon sector) rather than on the nightside. This matches the measured day/night asymmetry of lightning as reported by *Mazany et al.* [2002]. Lightning is much more frequent on the dayside, but when it couples through into the plasmasphere, it will be much more confined in longitude than lightning on the nightside. The nightside distributions (Figure 8b) still show the peak average spectral power density corresponding to land, but they are broader in longitudinal extent, showing less of a correspondence to land than on the dayside (Figure 8a) as would be expected from the transmitter analogy (Figure 4).

[42] The intensity of plasmaspheric hiss has been observed to be higher near the magnetic equator during substorm conditions [*Larkina and Likhter*, 1982]. The results of this study show that no significant changes in the latitudinal distribution of plasmaspheric hiss occur (see Figure 2a) whether IMF B_z, the substorm parameter that we chose to use, is positive or negative. Therefore this effect is not obvious in the wave map technique used in this study since average electric field spectra were used here. This implies that the mechanism responsible for the increase in the storm time hiss intensities (most likely the Kennel-Petschek mechanism) must be operating primarily in the slot region all the time at some level. During quiet periods the radiation belts come into equilibrium with the plasmaspheric hiss, revealing a slot region between the two Van Allen belts. However, during very strong geomagnetic storms this slot region can be filled with energetic particles. Even with the constant supply of lightning providing wave energy for the resonance interaction it can take up to 3 or more days for the belts to recover their normal equilibrium of a two-belt configuration.

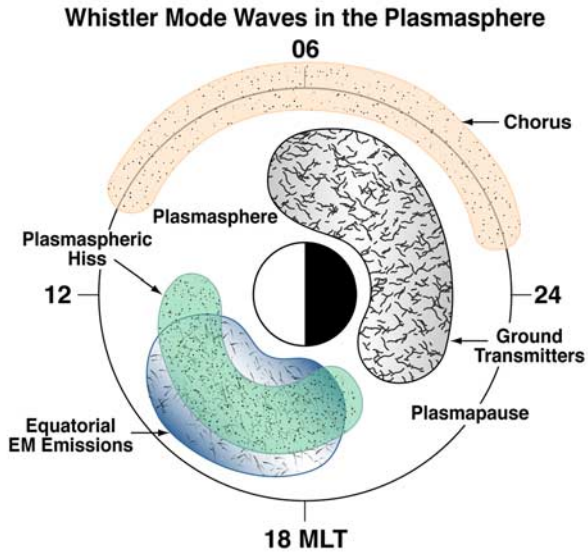

Figure 9. A summary of the local time distribution of the most intense portions of equatorial EM emissions, plasmaspheric hiss, and ground transmitters.

[43] Electrons, in the energy range from 100 to 300 keV, have been observed by the stimulated emission of energetic particles (SEEP) experiment on the S81-1 satellite to precipitate by lightning-generated whistlers as reported by *Voss et al.* [1984, 1998] and *Inan et al.* [1989]. More recently, *Abel and Thorne* [1998a, 1998b] and *Rodger et al.* [2003] determined, from modeling calculations, that electrons in the ~50–150 keV energy range can precipitate out of the slot region (L = 2–2.4) through gyroresonance interaction with lightning-generated whistlers as the dominant wave. The whistler distribution used by *Rodger et al.* [2003] was based on lightning climatology maps from *Christian et al.* [2003]. For electron energies above this range, *Rodger et al.* [2003] believe that ground-based transmitters and plasmaspheric hiss should dominate over all other loss processes. The results of our study are consistent with these conclusions based on actual observations of the distribution of plasmaspheric hiss that has lightning as its origin.

5. Conclusions

[44] From the analysis of plasma wave intensity maps from the DE/PWI and IMAGE/RPI instruments this paper puts into context a number of previous observations and proposed generation mechanisms of whistler mode waves in the plasmasphere. The whistler mode spectrum in the plasmasphere contains three basic broadband waves: equatorial EM emissions (~30–330 Hz), plasmaspheric hiss (~330 Hz to 3.3 kHz), and ground transmitter radiation (~10–50 kHz). Each of these waves is easily distinguishable by its spatial distributions in both local time and longitude. Figure 9 is a summary of where these waves are most intense in local time.

[45] Observations of EM equatorial emissions show that the most intense region is near the magnetic equator in the noon to afternoon sector. This emission is enhanced during storm times as illustrated by its dependence on the IMF B_z (see Figure 1). The observed average magnetic field spectral densities have latitudinal distributions that are very different from plasmaspheric hiss and ground transmitters and show an almost exclusive plasmasphere origin with lightning having little, if anything, to do with the intensity of this emission.

[46] The mapping of plasmaspheric hiss over nearly its entire frequency range (starting at ~500 Hz to over 3 kHz) from L shells >1.5 to geographic longitudes shows a number of features identical to those of lightning. The most intense plasmaspheric hiss is mapped to Northern Hemispheric continents (weakest hiss over oceans) and is stronger on the dayside than on the nightside and stronger during the summer than during the winter. The difference in average hiss intensity between the land and ocean is greater than an order of magnitude and is therefore comparable to that of the distribution of lightning. In addition, from wave intensity maps the high-latitude/low-altitude distribution of plasmaspheric hiss is identical to that of known ground transmitters which clearly have an Earth origin. The above strong correlation between regions of lightning and regions of hiss makes it clear that lightning is an embryonic source for hiss as originally suggested by *Sonwalkar and Inan* [1989]. However, it is not possible to determine if lightning is the sole source of plasmaspheric hiss as proposed by *Draganov et al.* [1992].

[47] It is important to also note that a clear intensification of hiss also occurs near the magnetic equator where particle-wave interactions, most likely generated by the *Kennel and Petschek* [1966] mechanism, occur. With lightning maintaining the average hiss intensity in the slot region the Kennel-Petschek mechanism must increase the hiss intensity during storm conditions as has recently been discussed by *Larkina and Likhter* [1982] and *Meredith et al.* [2004].

[48] Ground transmitter waves have narrow bandwidths (typically <1 kHz) and couple through the ionosphere primarily on the nightside. From ~10 to 50 kHz, whistler mode waves, observed by IMAGE/RPI (bandwidth 300 Hz), greatly fill in the spectrum between nontransmitter frequencies, with the implication that some unknown process is broadening the spectrum.

[49] **Acknowledgments.** The authors gratefully acknowledge discussions with Umran Inan and Richard Thorne. The data used in this paper are from the National Space Science Data Center archive. NASA supported the work at the University of Massachusetts, Lowell, under subcontracts to Southwest Research Institute under contract NASW-97002. The authors would also like to acknowledge the reviewers for their excellent remarks and suggestions.

[50] Lou-Chuang Lee thanks Umran Inan and Vikas Sonwalkar for their assistance in evaluating this paper.

References

Abel, B., and R. M. Thorne (1998a), Electron scattering loss in Earth's inner magnetosphere: 1. Dominant physical processes, *J. Geophys. Res.*, *103*, 2385–2396.

Abel, B., and R. M. Thorne (1998b), Electron scattering loss in Earth's inner magnetosphere: 2. Sensitivity to model parameters, *J. Geophys. Res.*, *103*, 2397–2407.

André, R., F. Lefeuvre, F. Simonet, and U. S. Inan (2002), A first approach to model the low-frequency wave activity in the plasmasphere, *Ann. Geophys.*, *20*, 981–996.

Boardsen, S. A., D. L. Gallagher, D. A. Gurnett, W. K. Peterson, and J. L. Green (1992), Funnel-shaped, low-frequency equatorial waves, *J. Geophys. Res.*, *97*, 14,967–14,976.

Bortnik, J., U. S. Inan, and T. F. Bell (2003a), Frequency-time spectra of magnetospherically reflecting whistlers in the plasmasphere, *J. Geophys. Res.*, *108*(A1), 1030, doi:10.1029/2002JA009387.

Bortnik, J., U. S. Inan, and T. F. Bell (2003b), Energy distribution and lifetime of magnetospherically reflecting whistlers in the plasmasphere, *J. Geophys. Res.*, *108*(A5), 1199, doi:10.1029/2002JA009316.

Christian, H. J., et al. (2003), Global frequency and distribution of lightning as observed from space by the Optical Transient Detector, *J. Geophys. Res.*, *108*(D1), 4005, doi:10.1029/2002JD002347.

Church, S. R., and R. M. Thorne (1983), On the origin of plasmaspheric hiss: Ray path integrated amplification, *J. Geophys. Res.*, *88*, 7941–7957.

Draganov, A. B., U. S. Inan, V. S. Sonwalkar, and T. F. Bell (1992), Magnetospherically reflected whistlers as a source of plasmaspheric hiss, *Geophys. Res. Lett.*, *19*, 233–236.

Dunckel, N., and R. A. Helliwell (1969), Whistler mode emissions on the Ogo 1 satellite, *J. Geophys. Res.*, *74*, 6371–6385.

Green, J. L., and S. A. Boardsen (1999), Confinement of nonthermal continuum radiation to low latitudes, *J. Geophys. Res.*, *104*, 10,307–10,316.

Gurnett, D. A. (1976), Plasma wave interactions with energetic ions near the magnetic equator, *J. Geophys. Res.*, *81*, 2765–2770.

Hayakawa, M., and S. S. Sazhin (1992), Mid-latitude and plasmaspheric hiss: A review, *Planet. Space Sci.*, *40*, 1325–1338.

Helliwell, R. A. (1965), *Whistlers and Related Ionospheric Phenomena*, pp. 61–72, Stanford Univ. Press, Stanford, Calif.

Horne, R. B., N. P. Meredith, R. M. Thorne, D. Heynderickx, R. H. A. Iles, and R. R. Anderson (2003), Evolution of energetic electron pitch angle distributions during storm time electron acceleration to megaelectronvolt energies, *J. Geophys. Res.*, *108*(A1), 1016, doi:10.1029/2001JA009165.

Huang, C. Y., C. K. Goertz, and R. R. Anderson (1983), A theoretical study of plasmaspheric hiss generation, *J. Geophys. Res.*, *88*, 7927–7940.

Imhof, W., R. R. Anderson, J. Reagan, and E. Gaines (1981), The significance of VLF transmitters in the precipitation of inner belt electrons, *J. Geophys. Res.*, *86*, 11,225–11,234.

Inan, U. S., and R. Helliwell (1982), DE-1 observations of VLF transmitter signals and wave particle interactions in the magnetosphere, *Geophys. Res. Lett.*, *9*, 917–920.

Inan, U. S., M. Walt, H. D. Voss, and W. L. Imhof (1989), Energy spectra and pitch angle distributions of lightning-induced electron precipitation: Analysis of an event observed on the S81-1 (SEEP) satellite, *J. Geophys. Res.*, *94*, 1379–1401.

Kennel, C. F., and H. E. Petschek (1966), Limit on stably trapped particle fluxes, *J. Geophys. Res.*, *71*, 1–28.

Koons, H. C. (1981), The role of hiss in magnetospheric chorus emissions, *J. Geophys. Res.*, *86*, 6745–6754.

Koons, H. C., and J. L. Roeder (1990), A survey of equatorial magnetospheric wave activity between 5 and 8 R_E, *Planet. Space Sci.*, *38*, 1335–1341.

Larkina, V. I., and J. I. Likhter (1982), Storm-time variations of plasmaspheric ELF hiss, *J. Atmos. Terr. Phys.*, *44*, 415–423.

Lyons, L. R., R. M. Thorne, and C. F. Kennel (1972), Pitch angle diffusion of radiation belt electrons within the plasmasphere, *J. Geophys. Res.*, *77*, 3455–3474.

Mazany, R., S. Businger, S. I. Gutman, and W. Roeder (2002), A lightning prediction index that utilizes GPS integrated precipitable water vapor, *Weather Forecast.*, *17*, 1034–1047.

Meredith, N. P., R. B. Horne, A. D. Johnstone, and R. R. Anderson (2000), The temporal evolution of electron distributions and associated wave activity following substorm injections in the inner magnetosphere, *J. Geophys. Res.*, *105*, 12,907–12,917.

Meredith, N. P., R. B. Horne, R. H. A. Iles, R. M. Thorne, D. Heynderickx, and R. R. Anderson (2002), Outer zone relativistic electron acceleration associated with substorm-enhanced whistler mode chorus, *J. Geophys. Res.*, *107*(A7), 1144, doi:10.1029/2001JA900146.

Meredith, N. P., R. B. Horne, R. M. Thorne, D. Summers, and R. R. Anderson (2004), Substorm dependence of plasmaspheric hiss, *J. Geophys. Res.*, *109*, A06209, doi:10.1029/2004JA010387.

Reinisch, B. W., et al. (2000), The radio plasma imager investigation on the IMAGE spacecraft, *Space Sci. Rev.*, *91*, 319–359.

Rodger, C. J., M. A. Cilverd, and R. J. McCormick (2003), Significance of lightning-generated whistlers to inner radiation belt electron lifetimes, *J. Geophys. Res.*, *108*(A12), 1462, doi:10.1029/2003JA009906.

Russell, C. T., R. E. Holzer, and E. J. Smith (1969), OGO 3 observations of ELF noise in the magnetosphere: 1. Spatial extent and frequency of occurrence, *J. Geophys. Res.*, *74*, 755–777.

Russell, C. T., R. E. Holzer, and E. J. Smith (1970), OGO 3 observations of ELF noise in the magnetosphere: 2. The nature of the equatorial noise, *J. Geophys. Res.*, *75*, 755–768.

Santolik, O., D. A. Gurnett, J. S. Picket, M. Parrot, and N. Cornilleau-Wehrlin (2004), A microscopic and nanoscopic view of storm-time chorus on 31 March 2001, *Geophys. Res. Lett.*, *31*, L02801, doi:10.1029/2003GL018757.

Sazhin, S. S., and M. Hayakawa (1992), Magnetospheric chorus emissions: A review, *Planet. Space Sci.*, *40*, 681–697.

Shawhan, S. D., D. A. Gurnett, D. L. Odem, R. A. Helliwell, and C. G. Park (1981), The plasma wave and quasi-static electric field instrument (PWI) for Dynamics Explorer-A, *Space Sci. Instrum.*, *5*, 535–550.

Solomon, J., N. Cornilleau-Wehrlin, A. Korth, and G. Kremser (1988), An experimental study of ELF/VLF hiss generation in the Earth's magnetosphere, *J. Geophys. Res.*, *93*, 1839–1847.

Sonwalkar, V. S., and U. S. Inan (1989), Lightning as an embryonic source of VLF hiss, *J. Geophys. Res.*, *94*, 6986–6994.

Stix, T. H. (1992), *Waves in Plasmas*, pp. 27–28, Am. Inst. of Phys., College Park, Md.

Storey, L. R. O. (1953), An investigation of whistling atmospherics, *Philos. Trans. R. Soc. London, Ser. A*, *246*, 113–141.

Summers, D., R. M. Thorne, and F. Xiao (1998), Relativistic theory of wave-particle resonant diffusion with application to electron acceleration in the magnetosphere, *J. Geophys. Res.*, *103*, 20,487–20,500.

Taylor, W. W. L., and D. A. Gurnett (1968), The morphology of VLF emissions observed with the Injun 3 satellite, *J. Geophys. Res.*, *73*, 5615–5626.

Thorne, R. M., and R. B. Horne (1994), Landau damping of magnetospherically reflected whistlers, *J. Geophys. Res.*, *99*, 17,249–17,258.

Thorne, R. M., E. J. Smith, R. K. Burton, and R. E. Holzer (1973), Plasmaspheric hiss, *J. Geophys. Res.*, *78*, 1581–1595.

Thorne, R. M., S. R. Church, and D. J. Gorney (1979), On the origin of plasmaspheric hiss: The importance of wave propagation and the plasmapause, *J. Geophys. Res.*, *84*, 5241–5247.

Tsurutani, B. T., S. R. Church, and R. M. Thorne (1979), A search for geographic control on the occurrence of magnetospheric ELF emissions, *J. Geophys. Res.*, *84*, 4116–4124.

Tsyganenko, N. A. (1995), Modeling the Earth's magnetospheric magnetic field confined within a realistic magnetopause, *J. Geophys. Res.*, *100*, 5599–5612.

Vampola, A. (1977), VLF transmission induced slot electron precipitation, *Geophys. Res. Lett.*, *4*, 569–572.

Voss, H. D., W. L. Imhof, J. Mobilia, E. E. Gaines, J. B. Reagan, U. S. Inan, R. A. Helliwell, D. L. Carpenter, J. P. Katsufrakis, and H. C. Chang (1984), Lightning-induced electron precipitation, *Nature*, *312*, 740–742.

Voss, H. D., M. Walt, W. L. Imhof, J. Mobilia, and U. S. Inan (1998), Satellite observations of lightning-induced electron precipitation, *J. Geophys. Res.*, *103*, 11,725–11,744.

S. Boardsen, L3 Communications Analytics Division, NASA Goddard Space Flight Center, Code 6320, Greenbelt, MD 20771, USA.

S. F. Fung, Space Physics Data Facility, NASA Goddard Space Flight Center, Mail Code 632, Greenbelt, MD 20771, USA.

L. Garcia and W. W. L. Taylor, QSS Group, Inc., 4500 Forbes Boulevard, Lanham, MD 20706, USA.

J. L. Green, Space Science Data Operations Office, NASA Goddard Space Flight Center, Mail Code 630, Building 26, Greenbelt, MD 20771, USA. (james.green@nasa.gov)

B. W. Reinisch, Center for Atmospheric Research, University of Massachusetts, 600 Suffolk Street, Lowell, MA 01854, USA.